Hydride transfer during catalysis by dihydrofolate reductase from *Thermotoga maritima*

Giovanni MAGLIA, Masood H. JAVED and Rudolf K. ALLEMANN[1]

School of Chemical Sciences, University of Birmingham, Edgbaston, Birmingham B15 2TT, U.K.

DHFR (dihydrofolate reductase) catalyses the metabolically important reduction of 7,8-dihydrofolate by NADPH. DHFR from the hyperthermophilic bacterium *Thermotoga maritima* (TmDHFR), which shares similarity with DHFR from *Escherichia coli*, has previously been characterized structurally. Its tertiary structure is similar to that of DHFR from *E. coli* but it is the only DHFR characterized so far that relies on dimerization for stability. The midpoint of the thermal unfolding of TmDHFR was at approx. 83 °C, which was 30 °C higher than the melting temperature of DHFR from *E. coli*. The turnover and the hydride-transfer rates in the kinetic scheme of TmDHFR were derived from measurements of the steady-state and pre-steady-state kinetics using absorbance and stopped-flow fluorescence spectroscopy. The rate constant for hydride transfer was found to depend strongly on the temperature and the pH of the solution. Hydride transfer was slow (0.14 s^{-1} at 25 °C) and at least partially rate limiting at low temperatures but increased dramatically with temperature. At 80 °C the hydride-transfer rate of TmDHFR was 20 times lower than that observed for the *E. coli* enzyme at its physiological temperature. Hydride transfer depended on ionization of a single group in the active site with a pK_a of 6.0. While at 30 °C, turnover of substrate by TmDHFR was almost two orders of magnitude slower than by DHFR from *E. coli*; the steady-state rates of the two enzymes differed only 8-fold at their respective working temperatures.

Key words: hydride transfer, kinetics, stability, thermophile.

INTRODUCTION

Enzymes are generally believed to adopt structures of marginal stability and high sensitivity to environmental changes, such as elevated temperatures. However, thermophilic organisms have evolved to cope with extreme conditions. Their enzymes resist heat denaturation at high temperatures and their optimal activity is reached well above 70 °C. Because the enzymes of thermophilic and mesophilic organisms are often homologous and most of their physicochemical properties are similar, Arrhenius theory predicts that thermophilic enzymes should be as active as their mesophilic counterparts at low temperatures. However, they often show only little activity at low temperatures, an observation that cannot be explained by cold denaturation as these enzymes do not unfold at low temperatures [1]. Many thermophilic and mesophilic enzymes appear to display optimal activity at the edge of their stability ranges. The reason for this correlation of stability and activity is not well understood but may lie in the dynamic nature of the molecular events associated with enzyme catalysis. The increased activity of thermophilic enzymes at elevated temperatures would therefore result from their increased dynamic flexibility [2–5].

A wealth of kinetic and computational data is available for DHFRs (dihydrofolate reductases) from mesophilic organisms [6]. DHFR is necessary for cellular metabolism in both prokaryotes and eukaryotes. It catalyses the reduction of 7,8-dihydrofolate (H_2F) using NADPH as a cofactor. Several antineoplastic and antimicrobial drugs such as methotrexate and pyrimethamine act by inhibiting DHFR. Complete kinetic schemes for the enzymes from *Escherichia coli* [7] and human [8] have been determined. At neutral pH the steady-state kinetic turnover is limited by 5,6,7,8-tetrahydrofolate (H_4F) release from the mixed ternary complex DHFR–NADPH–5,6,7,8-tetrahydrofolate. At pH > 9 the hydride transfer becomes rate limiting [7].

Several lines of evidence have indicated the importance of dynamic properties of EcDHFR (*E. coli* DHFR) for its functional activity. The angle and the distance between hydride donor and acceptor have been shown to be critical determinants of the rate of hydride transfer both from the inspection of crystal structure data and from *ab initio* calculations [9–11]. The NMR-derived order parameters and molecular dynamics simulations for the complex of DHFR with folate or methotrexate identified three main regions of motion within three surface loops, namely the M20 loop (residues 14–24), the FG loop (residues 116–125) and the CD loop (residues 64–71) [12,13]. A series of site-directed-mutagenesis studies performed on residues in these loop regions showed that long-range effects influence the rate of hydride transfer. In particular, mutations in the FG loop, which is approx. 17 Å away from the active site, caused a significant decrease in the rate of hydride transfer suggesting that these distant residues change the global dynamics of the protein [14]. Classical molecular dynamics simulations identified strongly coupled motions of amino acid residues in the Michaelis complex of EcDHFR [15]. These correlated motions, which involved the mobile loops identified by NMR, disappeared in the product complex, implying that they might be linked to catalysis. A network of promoting motions has recently been identified which ranges from Asp-122 in the FG loop through Gly-15 and Ile-14 in the Met-20 loop to Phe-31 and involves both the hydride donor and acceptor [16].

The recent characterization of the X-ray structure of TmDHFR (DHFR from the hyperthermophile *Thermotoga maritima*; Figure 1) revealed that its tertiary structure was similar to that of the *E. coli* enzyme despite only 27 % sequence identity between the two enzymes [17]. However, unlike its mesophilic counterparts, TmDHFR forms stable homodimers. No isolated structured monomers could be detected either in equilibrium or during unfolding [18].

Abbreviations used: H_2F; 7,8-dihydrofolate; NADPD, (4*R*)-[^{2}H]NADPH; DHFR, dihydrofolate reductase; EcDHFR, *Escherichia coli* DHFR; TmDHFR, *Thermotoga maritima* DHFR.

[1] To whom correspondence should be addressed (e-mail r.k.allemann@bham.ac.uk).

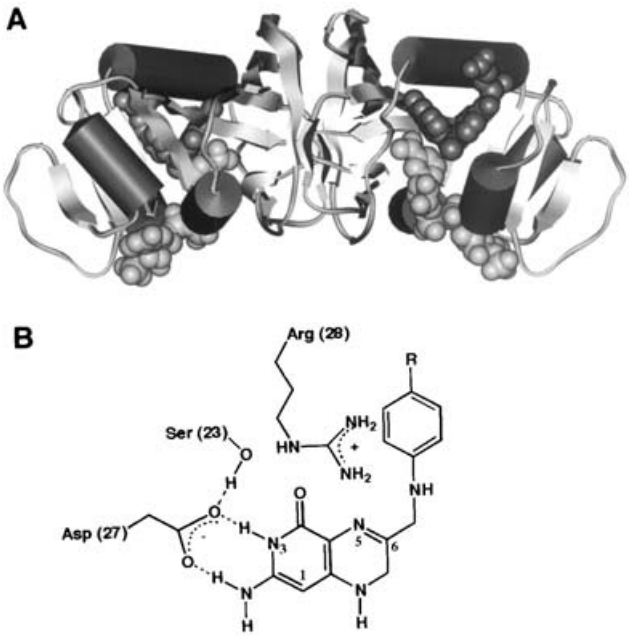

Figure 1 Structure of TmDHFR

(**A**) Ribbon diagram of the TmDHFR dimer [17]. Substrate and cofactor are depicted as space filling models. (**B**) The active site of TmDHFR taken from its X-ray structure [17].

The major contribution to the high thermal stability of TmDHFR was attributed to the interactions between the subunits, which involved regions equivalent to the FG loop in the *E. coli* enzyme [17]. The increased rigidity of the FG loop of TmDHFR might suggest a low kinetic activity at room temperature, which can be increased through higher dynamic motions at higher temperatures. We report here the results from kinetic measurements of the temperature dependence of both the hydride transfer and the steady-state turnover rates of the reduction of H_2F mediated by TmDHFR.

MATERIALS AND METHODS

Substrates and cofactors

H_2F was prepared by dithionite reduction of folate (Sigma) as described previously [19]. NADPH was purchased from Sigma. (4*R*)-[^{2}H]NADPH (NADPD) was prepared by reduction of $NADP^+$ (Sigma) using $NADP^+$-dependent alcohol dehydrogenase from *Thermoanaerobium brokii* (Sigma) [20] and purified by anion-exchange chromatography on Mono Q™ HR 5/5 (Amersham Biosciences) [21]. NADPH and NADPD concentrations were determined spectrophotometrically using an extinction coefficient of 6200 $cm^{-1} \cdot M^{-1}$ at 339 nm [7]. Similarly the concen–tration of H_2F was measured assuming an extinction coefficient of 28 000 $cm^{-1} \cdot M^{-1}$ at 282 nm for pH 7.4 [22].

Protein purification

A plasmid containing the cDNA for TmDHFR was a gift from Dr Nicolas Glansdorff (Research Institute, CERIA-COOVI, Brussels, Belgium) [23]. The cDNA was inserted between the *Nde*I and *Bam*HI restriction sites of pET11c and used for protein production in *E. coli* Codon Plus BL21(DE3) RP™ cells (Stratagene). Cells were grown at 37 °C to an attenuance at 600 nm of 0.6 in LB medium containing 0.27 mM ampicillin. Expression was induced by adding isopropyl D-β-thiogalactoside to a final concentration of 0.4 mM. Cells were harvested by centrifugation and resuspended in 50 mM Tris, pH 7/1 mM EDTA (100 ml/10 g of cells). The suspension was sonicated for 5 min, incubated with DNase (20 μg/ml), RNase (20 μg/ml) and $MgSO_4$ (20 mM) for 30 min and centrifuged. The protein was purified as described previously [24]. In short, the supernatant was diluted 4-fold and incubated at 78 °C for 20 min. The extract was cooled on ice for 5 min and centrifuged. The soluble fraction was applied to a HiPrep™ 16/10 SP XL cation-exchange column (Amersham Biosciences) and eluted with a gradient of 1 M NaCl in 50 mM Tris, pH 7/1 mM EDTA over 70 min. TmDHFR eluted around 200 mM NaCl and the buffer was exchanged to 10 mM phosphate buffer, pH 7. The protein was essentially pure as judged by SDS gel electrophoresis (Figure 2A). The mass of 19237 Da determined by electrospray ionization MS corresponded well to the calculated mass of 19236 Da. The protein concentration was measured spectrophotometrically ($\varepsilon_{280} = 22\,880\ cm^{-1} \cdot M^{-1}$) [24].

EcDHFR was produced and purified according to published procedures [14].

CD spectroscopy

All CD experiments were performed on a JASCO J810 spectrometer at a protein concentration of 1.2 μM in 10 mM K_2PO_4 (pH 7) and 200 mM KF. Protein unfolding was followed by monitoring the CD signal at 222 nm between 20 and 95 °C, applying a temperature gradient of 0.5 °C/min.

At a given temperature the fraction Φ of unfolded was calculated from the CD signal $[\Theta]_{222}$:

$$\Phi = \left([\Theta]^{F}_{222} - [\Theta]_{222}\right) \Big/ \left([\Theta]^{F}_{222} - [\Theta]^{U}_{222}\right),$$

where $[\Theta]^{F}_{222}$ and $[\Theta]^{U}_{222}$ are the CD signals obtained from the baseline extrapolation before and after the unfolding transition.

Steady-state kinetic measurements

Turnover rates were measured spectrophotometrically by following the decrease in absorbance at 340 nm during the reaction [ε_{340} (NADPH + DHF) = 13 200 $M^{-1} \cdot cm^{-1}$] [25]. The temperature was varied from 25 to 75 °C at pH 7. In a typical experiment the enzyme (10 μM) was preincubated with NADPH (50 μM) to avoid hysteresis. Enzyme–NADPH solution (10 μl) was added to 970 μl of MTEN buffer (25 mM Tris/25 mM ethanolamine/50 mM Mes/100 mM NaCl). Then 10 μl of NADPH (100 μM final concentration) was added to the solution and the reaction was started by adding 10 μl of H_2F (100 μM final concentration). The temperature of the reaction was controlled carefully by prewarming the buffer and utilizing a temperature-controlled cuvette holder. The extinction coefficient of NADPH is temperature-dependent and a correction factor of -0.13 %/1 °C rise in temperature was applied for ε_{340} [26].

For pH experiments MTEN buffer was used between pH 3 and 9. The reactions were run at 40 °C due to the low stability of substrate and cofactor at low pH and high temperature. All enzymic reaction rates were corrected for the non-enzymic decay of NADPH and H_2F.

Pre-steady-state kinetic measurements

Pre-steady-state kinetics experiments were performed on an Applied Photophysics stopped-flow spectrophotometer. Hydride-transfer rates were measured following the fluorescence energy

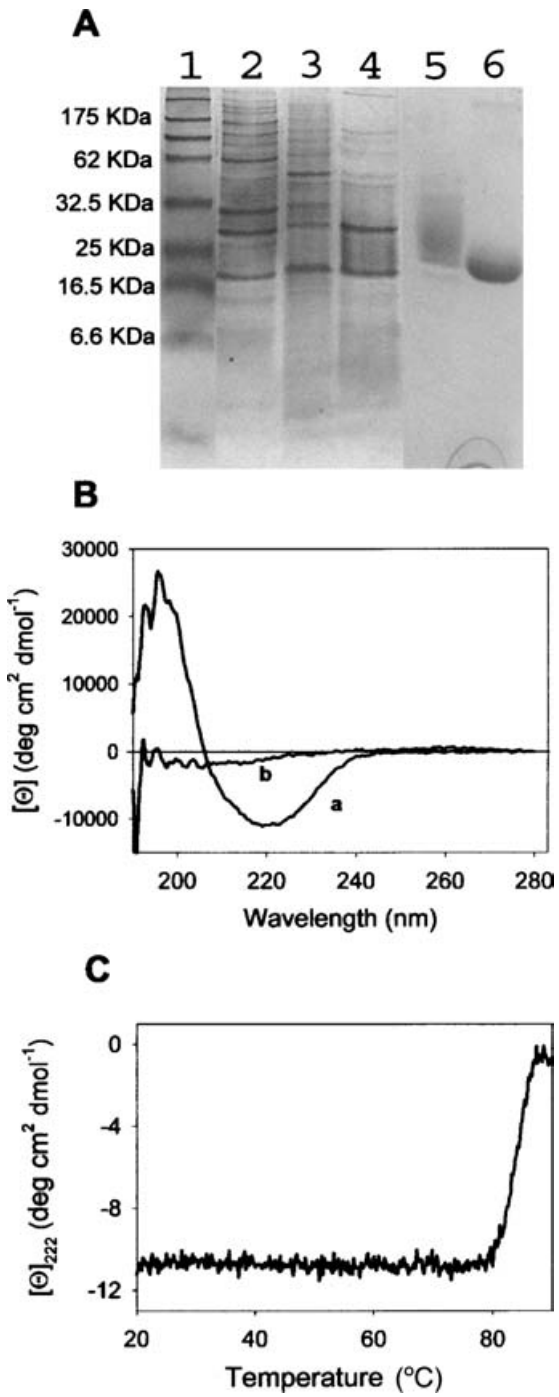

Figure 2 Characterization of TmDHFR

(**A**) SDS/PAGE gel showing the purification steps for TmDHFR produced in *E. coli* Codon Plus BL21(DE3) RP^{TM} cells as described in the Materials and methods section: lane 1, molecular-mass markers; lane 2, soluble fraction; lane 3, insoluble fraction after heat treatment at 78 °C for 20 min; lane 4, soluble fraction after heat treatment; lane 5, eluate from SP-Sepharose; lane 6, reconstituted fraction 5 after urea denaturation. (**B**) CD spectra of TmDHFR (1.2 μM) at 20 °C (trace a) and 90 °C (trace b) in 10 mM KPO_4 (pH 7), 200 mM KF. (**C**) The effect of temperature on the secondary structure of TmDHFR by monitoring the CD signal at 222 nm as a function of temperature. Conditions as described for (**B**).

transfer from the protein to reduced NADPH. The sample was excited at 290 nm and the emission measured using a 400 nm output filter. In a typical experiment, DHFR (40 μM) was pre-incubated with NADPH or NADPD (10 μM) in MTEN buffer and rapidly mixed with H_2F (200 μM) in the same buffer. A typical experiment is shown in Figure 4 (see below). These data fit well to a single exponential expression.

RESULTS AND DISCUSSION

Production of TmDHFR

Attempts to produce TmDHFR in *E. coli* BL21(DE3) cells led to the isolation of only small amounts of protein. A total of 11 Arg residues are encoded by nine AGA and two AGG codons in the cDNA for TmDHFR, while one CCA and two CCC codons are used for Pro [23]. The corresponding tRNAs are of low abundance in *E. coli* [27] and TmDHFR was therefore produced in *E. coli* Codon Plus BL21(DE3) RP^{TM} cells, which contain extra copies of the *argU* and *proL* tRNA genes allowing the production of 20 mg of pure protein from 1 l of culture.

Rather than a distinct band for a protein of the molecular mass of TmDHFR, a poorly focused region was detected by gel electrophoresis (Figure 2A). The crude protein mixture was heated to 78 °C for 20 min followed by rapid cooling on ice. This led to the precipitation of the majority of *E. coli* proteins whereas TmDHFR remained soluble due to its high temperature stability. PAGE of the soluble fraction revealed two bands at approx. 19 and 31 kDa. It had been reported previously that TmDHFR was resistant to denaturation by SDS [28]. The two bands most likely corresponded to the monomer and dimer of the enzyme since denaturation of the fully purified protein in 8 M urea led to a single band of molecular mass 19.5 kDa on SDS/PAGE (Figure 2A).

Temperature-induced unfolding

The CD spectrum of recombinant TmDHFR showed a minimum at 221 nm and a maximum at 196 nm (Figure 2B). In good agreement with the values published previously [18,24], the mean residue ellipticities at 222 and 196 nm were $-11\,000$ and $26\,100\ \mathrm{deg \cdot cm^2 \cdot dmol^{-1}}$ respectively, suggesting that the recombinant protein adopted the proper secondary and tertiary structures. The thermal stability of TmDHFR was measured by monitoring the CD spectrum as a function of temperature. The thermal unfolding profiles exhibited small linear variations of the signal between 20 and 77 °C corresponding to native baselines, a very sharp co-operative unfolding reaction and unfolded baseline regions at temperatures greater than 85 °C (Figure 2C). The midpoint of the transition was at 83 °C, which is approx. 30 °C higher than the melting temperature for EcDHFR [29] and the highest melting point for any DHFR studied so far. Interestingly, the thermal denaturation was not reversible due to precipitation of the denatured protein.

Steady-state kinetics

The steady-state rate of the reduction of H_2F by NADPH catalysed by TmDHFR at pH 7 increased in a sigmoidal fashion with temperature (Figure 3A and Table 1). The turnover rate was maximal at 75 °C (4.05 s^{-1}), which corresponded to the maximal experimental temperature. This temperature was only slightly below the optimal growth temperature of *T. maritima* [30]. At the respective optimal growth temperatures of 37 and 80 °C the steady-state rate of TmDHFR (approx. 4.8 s^{-1}) was approx. eight times slower than that of the *E. coli* enzyme (approx. 37 s^{-1}) [7].

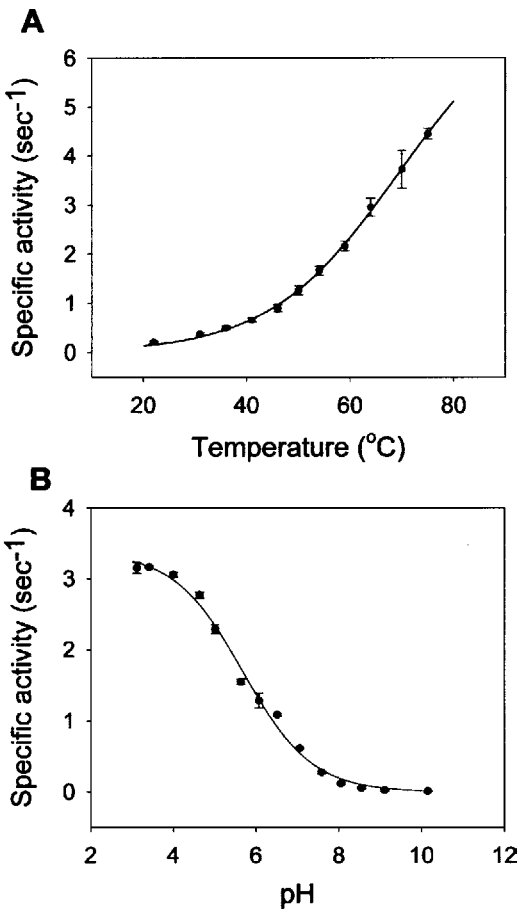

Figure 3 Steady-state kinetics of the TmDHFR-catalysed reduction of dihydrofolate by NADPH

Effect of temperature (**A**) and pH (**B**) on the specific activity of TmDHFR. Reactions were initiated by adding the enzyme (100 nM) previously pre-incubated with NADPH (500 nM), NADPH (100 μM) and H_2F (100 μM) in this order. The buffer was MTEN buffer (see text). The temperature was varied from 20 to 75 °C (pH 7) and the pH from 3 to 10 (40 °C).

Table 2 pH dependence of the reaction rates for hydride transfer and steady-state turnover during catalysis by TmDHFR in MTEN buffer at 40 °C

Steady-state rates are for the dimer of TmDHFR. nd, not determined.

pH	Hydride-transfer rate (s^{-1})	Steady-state rate (s^{-1})
9.0	0.023 ± 0.002	0.024 ± 0.015
8.5	0.059 ± 0.003	0.058 ± 0.015
8.0	0.15 ± 0.002	0.12 ± 0.03
7.5	0.31 ± 0.05	0.28 ± 0.02
7.0	0.52 ± 0.03	0.61 ± 0.04
6.5	1.57 ± 0.14	1.09 ± 0.02
6.0	3.06 ± 0.04	1.29 ± 0.13
5.5	3.89 ± 0.21	1.55 ± 0.03
5.0	6.22 ± 0.28	2.29 ± 0.26
4.5	nd	2.27 ± 0.05
4.0	nd	3.05 ± 0.38
3.5	nd	3.15 ± 0.1
3.0	nd	3.16 ± 0.2

When NADPD was used as a cofactor, an isotope effect of 3.5 was measured for the steady-state rate. This value was similar to that reported for EcDHFR above pH 9 [31], where hydride transfer was rate limiting. The increase in the steady-state reaction rate for EcDHFR was also found to be sigmoidal up to approx. 45 °C (results not shown). Above this temperature the reaction rate decreased due to the reversible denaturation of the enzyme.

The steady-state rates for TmDHFR catalysis were found to depend on the pH of the solution in a sigmoidal fashion at 40 °C (Figure 3B and Table 2). The temperature of 40 °C was chosen for the pH studies as a compromise between the instabilities of the cofactor and the substrate [$t_{1/2}$ (NADPH) ≈ 2 min at pH 3 and 40 °C] and the optimal working temperature of the enzyme. While the observed rates were slow above pH 7.5 (0.024 s^{-1} at pH 9), a rapid increase was observed below that value and the maximal rate of 3.16 s^{-1} was reached for pH values below 4. Changing the pH therefore led to more than a 100-fold variation in rate.

Table 1 Temperature dependence of the reaction rates for hydride transfer and steady-state turnover during catalysis by TmDHFR and EcDHFR in MTEN buffer at pH 7.0

Steady-state rates for TmDHFR are for the dimer of TmDHFR. nd, not determined.

	TmDHFR		EcDHFR	
Temperature (°C)	Hydride-transfer rate (s^{-1})	Steady-state rate (s^{-1})	Hydride-transfer rate (s^{-1})	Steady-state rate (s^{-1})
15	nd	nd	144.3 ± 11.1	8.5 ± 1.2
20	nd	nd	151.8 ± 20.3	12.6 ± 1.4
25	0.14 ± 0.01	0.20 ± 0.02	222.8 ± 1.3	16.4 ± 3.6
30	0.20 ± 0.02	0.35 ± 0.02	275.0 ± 4.5	24.0 ± 3.0
35	0.33 ± 0.03	0.47 ± 0.04	308.0 ± 2.2	32.03 ± 5.0
40	0.52 ± 0.03	0.61 ± 0.04	303.0 ± 3.3	44.9 ± 6.1
45	0.84 ± 0.13	0.83 ± 0.07	223.8 ± 7.4	53.9 ± 5.6
50	1.38 ± 0.19	1.17 ± 0.07	nd	nd
55	2.07 ± 0.16	1.53 ± 0.09	nd	nd
60	3.11 ± 0.21	2.00 ± 0.16	nd	nd
65	4.50 ± 0.41	2.70 ± 0.14	nd	nd
70	≈6.9*	3.40 ± 0.28	nd	nd
75	≈10.5*	4.05 ± 0.39	nd	nd
80	≈15.5*	≈4.8*	nd	nd

* Extrapolated data.

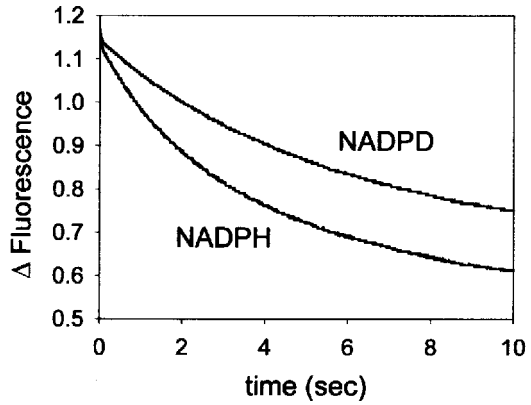

Figure 4 Stopped-flow fluorescence energy-transfer experiment of TmDHFR-catalysed hydride transfer from NADPH and NADPD to dihydrofolate

The enzyme (40 μM) was preincubated with NADPH or NADPD (10 μM) in MTEN buffer and the reaction was initiated by the addition of an equal volume of H_2F (200 μM). The buffer used was MTEN (pH 7) and the reaction temperature was 40 °C.

The inversion point was approx. 6, similar to that observed for the hydride-transfer rate (see below). The protonation state appeared therefore to be important for the reaction.

Pre-steady-state experiments

Due to the overlap of the emission spectrum of TmDHFR at 340 nm with the excitation maximum of the reduced cofactor, stopped-flow fluorescence could be used to measure the rate of the hydride-transfer step for DHFRs from *T. maritima* and *E. coli*. In a typical experiment 40 μM DHFR was incubated with 10 μM NADPH and then mixed with a large excess of substrate (200 μM). The change in fluorescence was followed as a function of time and fit to a single exponential expression for both enzymes (Figure 4). The reaction catalysed by TmDHFR occurred at a rate of 0.2 s^{-1} at neutral pH and 30 °C, which was three orders of magnitude slower than the corresponding rate for the *E. coli* enzyme at the same temperature (Table 1).

The rate of the hydride-transfer step was found to be strongly dependent on the temperature (Figure 5A and Table 1). Because of the limitations of the stopped-flow apparatus used, the maximal reaction temperature studied was 65 °C. The hydride transfer rates for TmDHFR increased exponentially with the temperature in the experimentally accessible range. Extrapolation by fitting an exponential graph to the data resulted in an estimated value of approx. 15.5 s^{-1} for the hydride transfer rate at 80 °C (Figure 4 and Table 1). For the *E. coli* enzyme the rate of the hydride transfer step increased linearly up to physiological temperature (Table 1). The rate measured for the hydride-transfer at 25 °C (222.8 s^{-1}) corresponded well with the rate published previously [7]. At higher temperatures a sharp decrease in the rate of the chemical step was observed as a consequence of the unfolding of the protein (Table 1).

The hydride-transfer rates for TmDHFR at the lower end of the temperature range were similar to the steady-state turnover rates (Table 1). The hydride-transfer step was therefore at least partly rate limiting in the catalytic cycle of TmDHFR below 50 °C. This behaviour was in sharp contrast to the *E. coli* enzyme where the hydride-transfer step at pH 7 was more than one order of magnitude faster than the steady-state rate [7]. For EcDHFR product release has been observed to be rate determining at physiological pH. Above 50 °C the hydride-transfer rate for TmDHFR

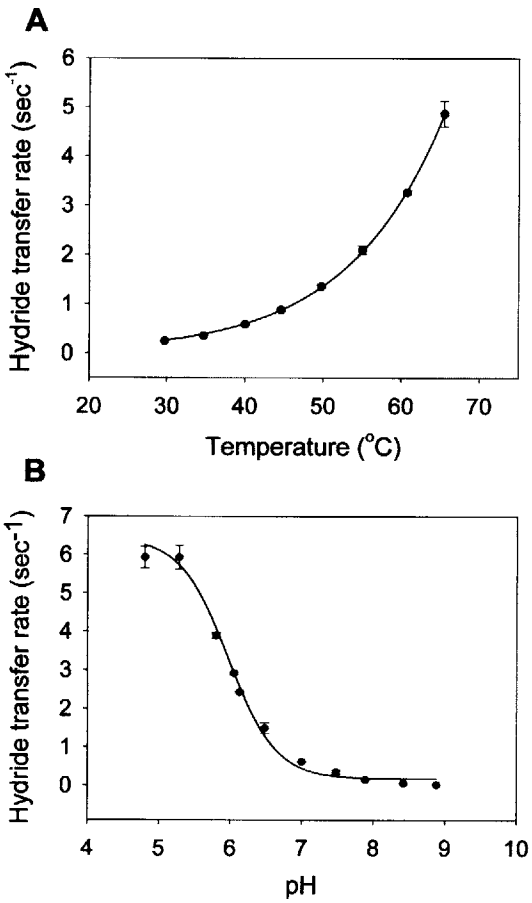

Figure 5 Pre-steady-state kinetics of the TmDHFR-catalysed hydride transfer from NADPH to dihydrofolate

Effect of temperature (**A**) and pH (**B**) on the hydride transfer of TmDHFR. Conditions were as in Figure 4. The temperature was varied from 20 to 65 °C and the pH from 10 to 4.

was significantly higher than the steady-state rate, indicating that hydride transfer was no longer rate determining.

The logarithm of the hydride-transfer rates for TmDHFR depended linearly on the inverse of the absolute temperature, indicating that the hydride-transfer reaction followed an Arrhenius-type temperature profile. From the Arrhenius plot, values of 75.6 ± 0.4 kJ · mol^{-1} and $(2.64 \pm 0.05) \times 10^{12}$ s^{-1} were obtained for the activation energy and the pre-exponential factor, respectively. As expected, the activation energy for the hydride transfer within the active site of TmDHFR was more than twice the value measured for the catalytically more efficient EcDHFR (28.2 ± 0.9 kJ · mol^{-1}; Table 1).

When the pre-steady-state experiments were repeated using 10 μM NADPD rather than NADPH (Figure 4) a temperature-independent kinetic isotope effect for the hydride transfer of 3.35 ± 0.23 was measured for TmDHFR, which was similar to the kinetic isotope effect reported for the *E. coli* enzyme [7].

Hydride transfer showed a strong dependence on pH. The hydride-transfer rate decreased with increasing pH (Figure 5B and Table 2). Comparison of the hydride-transfer rates with the steady-state transfer rates of TmDHFR showed that hydride transfer was rate limiting at high pH similar to the *E. coli* enzyme, where the rate of hydride transfer rapidly decreased with increasing pH, making it the rate-determining step above pH 9 [7]. The dependence of the rate constant for the hydride transfer

of TmDHFR on pH was well described by a single pH-dependent step with an apparent pK_a of approx. 6.0 (Figure 5B). The maximal rate at low pH (< 5) was 6.22 s^{-1} at 40 °C (Table 2). At this pH the *E. coli* enzyme was inactive due to pH-induced denaturation [32]. The pK_a observed in the pre-steady-state measurements of TmDHFR catalysis most likely represents the true pK_a of the ternary enzyme complex (TmDHFR.H_2F.NADPH). In the *E. coli* enzyme a pK_a for the reaction of 6.5 has been defined [6,7]. The pK_a of 6.5 has been attributed previously to Asp-27 [6], which is over 5 Å from N5 of H_2F and forms hydrogen bonds with the 2-amino and 3-NH groups of the pterin ring of the substrate in all DHFRs studied so far (Figure 1B). However, for the DHFRs from *Lactobacillus casei* [33], human [34] and cow [35] Asp-27 has been shown to remain unprotonated. The pK_a of 6.5 is therefore most likely due to the protonation of N5 of H_2F. The lower pK_a observed during TmDHFR catalysis as compared with EcDHFR might be a consequence of the proximity of Arg-28 in the active site of the thermophilic enzyme (Figure 1B). The positively charged guanidinium group should depress the pK_a of the protonated substrate relative to the *E. coli* enzyme where the equivalent residue is a leucine. In addition, the active site of TmDHFR appears from the X-ray structure [17] to be more solvent exposed than was observed in the *E. coli* enzyme [11] leading to a depression of the pK_a of protonated dihydrofolate towards its solution pK_a of 2.6 [36].

In summary, the catalytic properties of TmDHFR depended on the physical conditions of the reaction. At pH 7 hydride transfer was at least partially rate limiting for temperatures below 50 °C, whereas for higher temperatures hydride transfer was faster than the steady-state rate. At its physiological temperature the overall rate of TmDHFR catalysis was not determined by hydride transfer and it is plausible that at these high temperatures product release may be the slow step in the catalytic cycle, as was observed for EcDHFR [7]. Hydride-transfer and steady-state rates during TmDHFR catalysis were relatively slow when compared with mesophilic DHFRs at their respective physiological temperatures (EcDHFR was 20 times faster for hydride transfer, but only approx. 8 times faster in the steady state). Whereas there were differences in detail, the overall kinetic behaviour of TmDHFR was similar to that of the *E. coli* enzyme except for the higher rate accelerations observed with the *E. coli* enzyme. Catalysis by both enzymes depended on a single pK_a of approx. 6. The catalytic efficiency increased with decreasing pH and with increasing temperature. The maximal activity was reached around the respective physiological temperatures, which could be a consequence of the different dynamic properties of the two enzymes. TmDHFR has evolved to maintain a stable three-dimensional structure at temperatures well above the melting temperature of the *E. coli* enzyme. The basis of this extraordinary stability appears to be to a large extent the formation of homodimers between TmDHFR subunits [17,18]. A consequence of this increased stability is enhanced rigidity, which in turn might be the basis of the reduced activity of TmDHFR at mesophilic temperatures. Experiments are currently underway to determine the temperature dependence of the vibrational flexibilities of DHFRs from *E. coli* and *T. maritima*.

We thank Nicolas Glansdorff for providing us with a cDNA for DHFR from *T. maritima* and Paul Shrimpton for helpful discussions and critical reading of the manuscript. This work was supported by the BBSRC and the University of Birmingham (Ph.D. studentship to G. M.)

REFERENCES

1 Jaenicke, R. (1991) Protein stability and molecular adaptation to extreme conditions. Eur. J. Biochem. **202**, 715–772

2 Zavodszky, P., Kardos, J., Svingor, A. and Petsko, G. A. (1998) Adjustment of conformational flexibility is a key event in the thermal adaptation of proteins. Proc. Natl. Acad. Sci. U.S.A. **95**, 7406–7411

3 Jaenicke, R. (2000) Do ultrastable proteins from hyperthermophiles have high or low conformational rigidity? Proc. Natl. Acad. Sci. U.S.A. **97**, 2962–2964

4 Kohen, A. and Klinman, J. P. (2000) Protein flexibility correlates with degree of hydrogen tunneling in thermophilic and mesophilic alcohol dehydrogenase. J. Am. Chem. Soc. **122**, 10738–10739

5 Svingor, A., Kardos, J., Hajdú, I., Németh, A. and Závodszky, P. (2001) A better enzyme to cope with cold. Comparative flexibility studies on psychrotrophic, mesophilic and thermophilic IPMDHS. J. Biol. Chem. **276**, 28121–28125

6 Miller, G. P. and Benkovic, S. J. (1998) Stretching exercises – flexibility in dihydrofolate reductase catalysis. Chem. Biol. **5**, R105–R113

7 Fierke, C. A., Johnson, K. A. and Benkovic, S. J. (1987) Construction and evaluation of the kinetic scheme associated with dihydrofolate reductase from *Escherichia coli*. Biochemistry **26**, 4085–4092

8 Appleman, J. R., Beard, W. A., Delcamp, T. J., Prendergast, N. J., Freisheim, J. H. and Blakely, R. L. (1990) Unusual transient-state and steady-state kinetic behaviour is predicted by the kinetic scheme operational for recombinant human dihydrofolate reductase. J. Biol. Chem. **265**, 2740–2748

9 Wu, Y. D. and Houk, K. N. (1987) Theoretical transition structures for hydride transfer to methyleniminium ion from methylamine and dihydropyridine – on the nonlinearity of hydride transfers. J. Am. Chem. Soc. **109**, 2226–2227

10 Reyes, V. M., Sawaya, M. R., Brown, K. A. and Kraut, J. (1995) Isomorphous crystal structures of *Escherichia coli* dihydrofolate reductase complexed with folate, 5-deazafolate, and 5,10-dideazatetrahydrofolate – mechanistic implications. Biochemistry **34**, 2710–2723

11 Sawaya, M. R. and Kraut, J. (1997) Loop and subdomain movements in the mechanism of *Escherichia coli* dihydrofolate reductase: crystallographic evidence. Biochemistry **36**, 586–603

12 Epstein, D. M., Benkovic, S. J. and Wright, P. E. (1995) Dynamics of the dihydrofolate reductase folate complex – catalytic sites and regions known to undergo conformational change exhibit diverse dynamical features. Biochemistry **34**, 11037–11048

13 Osborne, M. J., Schnell, J., Benkovic, S. J., Dyson, H. J. and Wright, P. E. (2001) Backbone dynamics in dihydrofolate reductase complexes: role of loop flexibility in the catalytic mechanism. Biochemistry **40**, 9846–9859

14 Cameron, C. E. and Benkovic, S. J. (1997) Evidence for a functional role of the dynamics of glycine-121 of *Escherichia coli* dihydrofolate reductase obtained from kinetic analysis of a site-directed mutant. Biochemistry **36**, 15792–15800

15 Radkiewicz, J. L. and Brooks, III, C. L. (2000) Protein dynamics in enzymatic catalysis: exploration of dihydrofolate reductase. J. Am. Chem. Soc. **122**, 225–231

16 Agarwal, P. K., Billeter, S. R., Rajagopalan, P. T. R., Benkovic, S. J. and Hammes-Schiffer, S. (2002) Network of coupled promoting motions in enzyme catalysis. Proc. Natl. Acad. Sci. U.S.A. **99**, 2794–2799

17 Dams, T., Auerbach, G., Bader, G., Jacob, U., Ploom, T., Huber, R. and Jaenicke, R. (2000) The crystal structure of dihydrofolate reductase from *Thermotoga maritima*: molecular features of thermostability. J. Mol. Biol. **297**, 659–672

18 Dams, T. and Jaenicke, R. (2001) Stability and folding of dihydrofolate reductase from the hyperthermopohilic bacterium *Thermotoga maritima*. Biochemistry **38**, 9169–9178

19 Blakeley, R. L. (1960) Crystalline dihydropteroglutamic acid. Nature (London) **188**, 231–232

20 Jeong, S. S. and Gready, J. E. (1994) A method of preparation and purification of (4R)-deuterated-reduced nicotinamide adenine dinucleotide phosphate. Anal. Biochem. **221**, 273–277

21 Orr, G. A. and Blanchard, J. S. (1984) High-performance ion-exchange separation of oxidized and reduced nicotinamide adenine dinucleotides. Anal. Biochem. **142**, 232–234

22 Dawson, R. M. C., Elliott, D. C., Elliott, W. H. and Jones, K. M. (1969) Data for Biochemical Research, Oxford University Press, Oxford

23 Van de Casteele, M., Legrain, C., Wilquet, V. and Glansdorf, N. (1995) The dihydrofolate reductase-encoding gene dyrA of the hyperthermophilic bacterium *Thermotoga maritima*. Gene **158**, 1101–1105

24 Dams, T. and Jaenicke, R. (2001) Dihydrofolate Reductase from *Thermotoga maritima*. Methods Enzymol. **331**, 305–317

25 Miller, G. P. and Benkovic, S. J. (1998) Deletion of a highly motional residue affects formation of the michaelis complex for *Escherichia coli* dihydrofolate reductase. Biochemistry **37**, 6327–6335

26 Walsh, K. A. J., Daniel, R. M. and Morgan, H. W. (1983) A soluble NADH dehydrogenase (NADH-ferric anide oxidoreductase) from *Thermus aquaticus* strain T351. Biochem. J. **209**, 427–433

27 Kane, J. F. (1995) Effects of rare codon clusters on high-level expression of heterologous proteins in *Escherichia coli*. Curr. Opin. Biotechnol. **6**, 494–500
28 Wilquet, V., Gaspar, J. A., van de Lande, M., van de Casteele, M., Legrain, C., Meiering, E. M. and Glansdorff, N. (1998) Purification and characterisation of recombinant *Thermotoga maritima* dihydrofolate reductase. Eur. J. Biochem. **255**, 628–637
29 Ionescu, R. M., Smith, V. F., O'Neil, Jr, J. C. and Matthews, C. R. (2000) Multistate equilibrium unfolding of *Escherichia coli* dihydrofolate reductase: thermodynamic and spectroscopic description of the native, intermediate, and unfolded ensembles. Biochemistry **39**, 9540–9550
30 Huber, R., Langworthy, T. A., König, H., Thomm, M., Woese, C. R., Sleytr, U. B. and Stetter, K. O. (1986) *Thermotoga maritima* sp. nov. represents a new genus of unique extremely thermophilic eubacteria growing up to 90 °C. Arch. Microbial. **144**, 324–333
31 Chen, J.-T., Taira, K., Tu, C.-P. D. and Benkovic, S. J. (1987) Probing the functional role of phenylalanine-31 of *Escherichia coli* dihydrofolate reductase by site-directed mutagenesis. Biochemistry **26**, 4093–4100
32 Ohmae, E., Kurumiya, T., Makino, S. and Gekko, K. (1996) Acid and thermal unfolding of *Escherichia coli* dihydrofolate reductase. J. Biochem. (Tokyo) **120**, 946–953
33 Casarotto, M. G., Basran, J., Badii, R., Sze, K. H. and Roberts, G. C. K. (1999) Direct measurement of the pK_a of apartic acid 26 in *Lactobacillus casei* dihydrofolate reductase: implications for the catalytic mechanism. Biochemistry **38**, 8038–8044
34 Blakley, R. L., Appleman, J. R., Freisheim, J. H. and Jablonsky, M. J. (1993) Nuclear magnetic resonance evidence that the active site carboxyl group of dihydrofolate reductase is not involved in the relay of a proton to substrate. Arch. Biochem. Biophys. **306**, 501–509
35 Selinsky, B. S, Perlman, M. E., London, R. E., Unkefer, C. J., Mitchell, J. and Blakley, R. L. (1990) C13 and N15 nuclear magnetic resonance evidence of the ionisation state of substrates bound to bovine dihydrofolate reductase. Biochemistry **29**, 1290–1296
36 Mahrai, G., Selinsky, B. S., Appleman, J. R., Perlman, M., London, R. E. and Blakley, R. A. (1990) Dissociation-constants for dihydrofolic acid and dihydrobiopterin and implications for mechanistic models for dihydrofolate reductase. Biochemistry **29**, 4554–4560

Received 17 March 2003/6 May 2003; accepted 23 May 2003
Published as BJ Immediate Publication 23 May 2003, DOI 10.1042/BJ20030412